A clock for solar and geomagnetic activity

Sandra C Chapman[1], Scott W McIntosh[2], Robert J. Leamon[3], and Nicholas Wynn Watkins[4]

[1]University of Warwick
[2]HAO/NCAR
[3]University of Maryland
[4]LSE

November 22, 2022

Abstract

The frequency of major solar eruptions, and their space weather impacts at earth vary with the cycle of solar activity but large amplitude events can occur at any time. Each solar cycle has a distinct amplitude and duration so that the solar cycle dependent frequency of rare, extreme space weather events is challenging to quantify. By constructing the analytic signal of daily sunspot numbers since 1818 we construct a new solar cycle phase clock which maps each of the last 18 solar cycles onto a single time-base. This clock orders solar coronal activity and extremes of the aa index, which tracks geomagnetic storms at the earth's surface over the last 14 solar cycles. We identify and quantify the occurrence times of a geomagnetically quiet solar cycle interval of ~4.4 years (~2 pi/5 phase or 40% of the cycle) in extent centered on solar minimum within which only two severe (aa>300nT) and one extreme (aa>500nT) geomagnetic storms occurred since 1868. The solar cycle modulation of activity is such that 1-3% of severe (aa>300nT) geomagnetic storms and 4-6% of C, M and X class solar flares occurred in the solar cycle quiet phase. Terminators of solar EUV bright point activity indicate the end of this quiet interval and the 'switch on' of increased frequency of solar flares and geomagnetic storms. This provides quantitative support to planning resilience against space weather impacts since only a few percent of all severe storms occur in this quiet interval and its start and end are forecast-able.

Posted on 22 Nov 2022 — The copyright holder is the author/funder. All rights reserved. No reuse without permission. — https://doi.org/10.1002/essoar.10501639.1 — This a preprint and has not been peer reviewed. Data may be preliminary.

A clock for solar and geomagnetic activity

S. C. Chapman[1], **S.W.McIntosh**[2], **R. J. Leamon**[3,4], **N. W. Watkins**[1,5,6]

[1]Centre for Fusion, Space And Astrophysics, Physics Department, University of Warwick, Coventry CV4 7AL
[2]National Center for Atmospheric Research, P.O. Box 3000, Boulder, CO 80307, USA.
[3]University of Maryland, Department of Astronomy, College Park, MD 20742, USA.
[4]NASA Goddard Space Flight Center, Code 672, Greenbelt, MD 20771, USA.
[5]Centre for the Analysis of Time Series, London School of Economics and Political Science, London, WC2A 2AZ, UK
[6]Faculty of Science, Technology, Engineering and Mathematics, The Open University, Milton Keynes, MK7 6AA, UK

Key Points:

- New sun clock which maps each irregular solar cycle of activity onto a regular timebase
- Identify a quiet phase centred on solar minimum that is 40% of the cycle and has forecast-able start and end
- 1-3% of severe ($aa > 300nT$) geomagnetic storms and 4-6% of C, M and X class solar flares occurred in the solar cycle quiet phase

Corresponding author: S. C. Chapman, `S.C.Chapman@warwick.ac.uk`

Abstract

The frequency of major solar eruptions, and their space weather impacts at earth vary with the cycle of solar (sunspot) activity but large amplitude events can occur at any time. Each solar cycle has a distinct amplitude and duration so that the solar cycle dependent frequency of rare, extreme space weather events is challenging to quantify. By constructing the analytic signal of daily sunspot numbers since 1818 we construct a new solar cycle phase clock which maps each of the last 18 solar cycles onto a single timebase. This clock orders solar coronal activity and extremes of the *aa* index, which tracks geomagnetic storms at the earth's surface over the last 14 solar cycles. We identify and quantify the occurrence times of a geomagnetically quiet solar cycle interval of $\sim$ 4.4 years ($\sim 2\pi/5$ phase or 40% of the cycle) in extent centred on solar minimum within which only two severe ($aa > 300nT$) and one extreme ($aa > 500nT$) geomagnetic storms occurred since 1868. The solar cycle modulation of activity is such that 1-3% of severe ($aa > 300nT$) geomagnetic storms and 4-6% of C, M and X class solar flares occurred in the solar cycle quiet phase. Terminators of solar EUV bright point activity indicate the end of this quiet interval and the 'switch on' of increased frequency of solar flares and geomagnetic storms. This provides quantitative support to planning resilience against space weather impacts since only a few percent of all severe storms occur in this quiet interval and its start and end are forecast-able.

Plain Language Summary

Extreme space weather events or super-storms have a high impact over a wide range of systems, from power supplies, aviation, satellites and radio communications to economic and social behaviour. They are becoming increasingly important as our society relies more and more on being interconnected. Whilst it is well known that severe space weather activity is modulated by the solar cycle, the variable duration of the cycle has made this risk difficult to quantify and there is still the possibility of a severe event during solar minimum. The relative likelihood of severe space weather events at different phases of the solar cycle is a key result of this work. We map this irregular cycle in time onto a uniform solar cycle clock and find a quite strong solar cycle modulation, with only a few per cent of the most severe solar flares and space storms occurring during the minimum 'quiet' phase of the cycle, the timing of which we have identified. This has operational implications for the users of near earth space as well as power grid operators who need to schedule critical maintenance during periods of quiet space weather.

1 Introduction

Extreme space weather events can disrupt power distribution, aviation, communication and satellites. They are driven by large scale plasma structures emitted from the solar corona but the geoeffectiveness of an event depends on many factors, including how the event propagates from sun to earth and how it interacts with earth's magnetosphere [Hathaway, 2015; Baker & Lanzerotti, 2016]. Events that lead to geomagnetically induced currents that affect power grids are statistically more likely close to solar maximum and in the descending phase of the solar cycle, but importantly they also occur at all other times in the solar activity cycle [Thomson et al., 2010]. As the largest events can result in significant societal impact and financial loss [Hapgood, 2019; Oughton et al., 2017], quantifying the chance of occurrence of extreme space weather events is essential to planning the resilience of vulnerable systems to catastrophic failure.

When more frequent, moderate space weather storms are aggregated across different solar cycles, there is a well established correlation between occurrence rate and solar cycle modulated activity [Tsurutani et al., 2006; Tsubouchi & Omura, 2007]. However due to their rarity, the likelihood of more extreme geomagnetic storms is challenging to quantify and thus most estimates[Thomson et al., 2011] are averages over multiple solar cycles.

Estimates based on extrapolating a power law event distribution [Riley, 2012] suggest a 12% probability of a "Carrington Class" [Tsurutani et al., 2003] extreme event in the next solar cycle, but are highly uncertain, and an underlying solar cycle modulation would contribute to this uncertainty [Riley & Love, 2016]. Some estimates based on extreme value statistics [Thomson et al., 2011] suggest the probability can be much lower [Siscoe, 1976; Silbergleit, 1996, 1999; Tsubouchi & Omura, 2007; Elvidge & Angling, 2018].

Crucially, each solar cycle is unique in amplitude and duration (see e.g. Hathaway [2015]; Russell et al. [2019]) and geomagnetic activity tracks the different levels of activity of each solar maximum and declining phase [Chapman et al., 2018; Lockwood et al., 2018]. Quantifying how solar coronal activity, and the chance of an extreme space weather event, varies within each cycle and from one solar cycle to the next is central to space weather resilience planning. A uniform normalized time-base for the solar cycle is needed in order to collate data across solar cycles of different duration in order to quantify correlation between the frequency of occurrence of severe geomagnetic storms and solar cycle activity phase. In this Letter we propose a new solar cycle 'clock' which stretches (or shrinks) the observed sunspot cycle of activity onto a single (normalized 11 year) time-base. Once we have shown that this clock can be constructed, we find that it orders both the level of solar coronal activity, and severe geomagnetic activity as seen in the extremes of long-term geomagnetic indices such as the *aa* index [Mayaud, 1972, 1980] that is available over the last 151 years.

2 Constructing the Sun Clock

The daily sunspot number record provides an almost uninterrupted measure of solar coronal activity since 1818 and is plotted in Figure 1(a). We can see that both the amplitude and duration of each solar cycle varies from one cycle to the next. We will express this time series $S(t)$ in terms of a time-varying amplitude $A(t)$ and phase $\phi(t)$ by obtaining its analytic signal [Gabor, 1946; Boashash, 1992] $A(t)exp[i\phi(t)]$ such that the real part of this signal is $S(t)$ and the imaginary part is obtained such that $A(t)exp[i\phi(t)] = S(t) + iH(t)$ where $H(t)$ is the Hilbert transform of $S(t)$. This is a standard approach that is used to test for synchronisation (e.g. Chapman et al. [2018]) and for amplitude-frequency relationships [Palŭs & Notovná, 1999]. Here it is used to provide a mapping between time and signal phase, that converts the (variable) duration of each solar cycle into a corresponding uniform phase interval, from $0 - 2\pi$.

For a discrete signal such as the daily sunspot number analysed here, a discrete analytic signal can be constructed from the discrete Fourier transform of the original signal. We have used a standard method [Marple, 1999] which satisfies both invertability and orthogonality. While defined for an arbitrary time series, the analytic signal will only give a physically meaningful decomposition of the original time series if that the instantaneous frequency $\omega(t) = d\phi(t)/dt$ remains positive [Boashash, 1992]. We therefore need to remove fast fluctuations and, for a positive-definite signal such as the daily sunspot number, a background trend (see Chapman et al. [2018] for an example, and further discussions in Boashash [1992]). Before performing the Hilbert transform to obtain the analytic signal we first performed a 180 day moving average and obtained a slowly-varying trend by performing a robust local linear regression which down-weights outliers ('rlowess') using a 40 year window. Figure 1 charts how we construct the analytic signal for the daily sunspot record. We first subtract the long-timescale trend (the blue line in Figure 1(a)) to give a sunspot time series that is unambiguously zero-crossing (Figure 1(b)). We then obtain the Hilbert transform $H(t)$ for this (180 day moving average) smoothed and detrended signal which then gives the analytic signal. Figure 1 (c) and (d) plot $A(t)$ and $\phi(t)$ respectively. Each cycle maximum (red circles) and minimum (green circles) is also overplotted on the analytic phase.

Recently, cycle terminators [McIntosh et al., 2014a,b, 2019] have been identified based on multiple observations of coronal magnetic activity which indicate the end of one cycle of activity and the beginning of the next. The termination of a solar cycle, or terminator, has a three-component global signature [McIntosh et al., 2019]. It is initially observed as a very abrupt reduction in the density of EUV bright point density around the solar equator, marking the final cancellation of the old cycle's (magnetic) activity bands at the equator [McIntosh et al., 2014a]. The equatorial reduction occurs in close conjunction with a very rapid growth of bright point density in the (magnetic) activity bands at mid-latitudes. This switch in magnetic flux emergence patterns occurs at the same time as the rapid increase in the number of mid-latitude sunspots which belong to the new solar cycle. At higher solar latitudes, the terminator is signalled as the start of the polar magnetic reversal process [McIntosh et al., 2019], or the "rush to the poles" phenomenon [Babcock, 1961; Sheeley et al., 1989]. We may therefore expect terminators to feature significantly in how solar cycle activity is ordered. The terminator times [McIntosh et al., 2019] are plotted on Figure 1 (d) (blue circles). They are located between each solar cycle minimum and the maximum of the next cycle and we have chosen zero phase to be at the time of the last cycle (24) terminator as estimated by McIntosh et al. [2019].

We can use the mapping between time and phase shown in Figure 1(d) to construct a sun clock which for each solar cycle has a different duration in time, but which maps onto a regular $0 - 2\pi$ interval in phase. We will see how this orders observations that are available over multiple solar cycles. The F10.7 index (the solar radio flux at 10.7 cm, Tapping [2013]) is available since 1947 giving 6 solar cycles of observations. As well as providing an index of the state of the solar corona, it is used by many operational space weather models as their prime solar input. It is correlated with the density of the upper atmosphere which in turn has consequences for the design and operation of satellites in low earth orbit (e.g. Vedder et al. [1992]). The intensity and occurrence times of solar flares seen in X-ray have been continuously observed by GOES and these are catalogued since 1975, that is, over the last 4 solar cycles. The intensity of space weather events is routinely characterized by geomagnetic indices that are derived from ground based magnetometer observations [Mayaud, 1980]. The *aa* index is constructed [Mayaud, 1972] from the 3 hourly K indices determined at two antipodal observatories (invariant magnetic latitude 50 degrees) and is available over the last 14 solar cycles, from 1868 to the present. An important consideration is that the *aa* index (units, nT) is discretized in amplitude [Bubenik & Fraser-Smith, 1977; Chapman et al., 2019] since the underlying K index [Bartels et al., 1939] is a quasi-logarithmic 0-9 integer scale that characterizes the maximum positive and negative magnetic deviations that occur during each 3 hour period at a given observatory.

3 Results

3.1 Sun clocks for solar and geomagnetic activity

We map the last 18 solar cycles onto a regular $[0 - 2\pi]$ interval in phase to produce a phase clock as shown in Figures 2 and 3. On the inner ring of both figures we plot the minima and maxima of the last 18 cycles and the terminators of the last 12 cycles. Lines indicate the average of each of these, this forms the basis of the solar cycle clock which we can read off as having a (normalized) 11 year period corresponding to 2π in phase. Increasing time (phase) is read clockwise as plotted. We can now add to this phase clock multi-solar cycle observations of solar and geomagnetic activity. Solar flares catalogued from GOES X-ray flux observations are available for the last four solar cycles. Their occurrence is plotted as (scaled) counts in non-overlapping 3 month binned histograms in Figure 2, X-class, M-Class and C-class flare counts indicated by red, blue and green histogram bars respectively. In Figure 3, rings of red, blue and green dots indicate (non-overlapping) days in which X-class, M-Class and C-class flares respectively occurred. As we would expect, the occurrence of flares is modulated by the solar cycle. As the F10.7

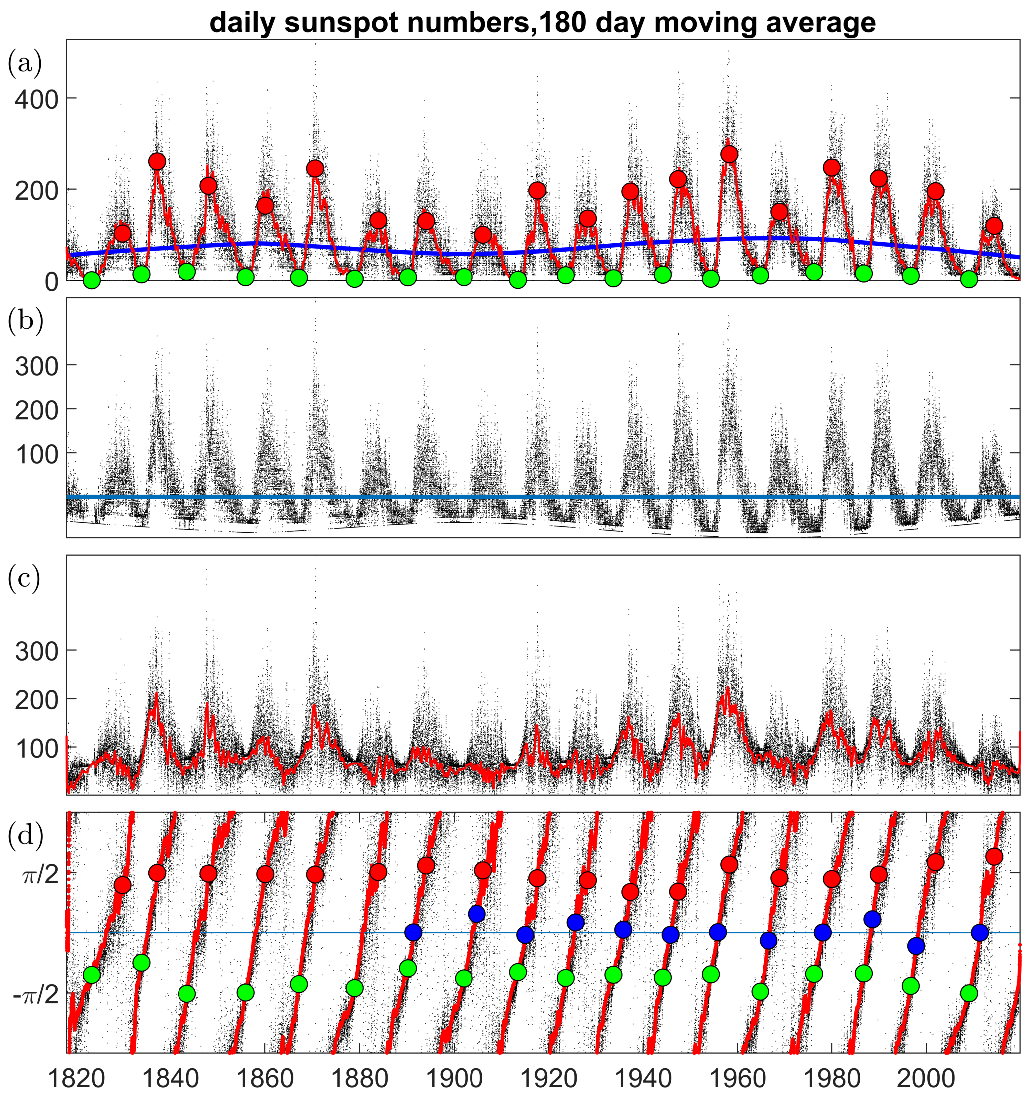

Figure 1. From top to bottom (a) Daily sunspot number (black), 180 day moving average (red) and slow timescale trend obtained by local regression using weighted linear least squares on a 40 year window (blue); (b) daily sunspot number with local regression trend subtracted; (c) analytic signal amplitude of monthly (black) and moving average (red) sunspot number; (d) analytic signal phase as in (c). On all panels the maxima and minima of the last 18 solar cycles are indicated by red and green circles respectively and the blue circles indicate terminators for the last 12 solar cycles obtained previously [McIntosh et al., 2019].

index is a well resolved time series we can directly obtain its analytic phase using the same method as for the daily sunspot number. Daily F10.7 observations are overplotted for the full 6 solar cycle record in Figure 2 (blue dots) and again are clearly ordered by the sun clock.

To see to what extent the solar cycle clock orders the geomagnetic space weather response seen at earth, in Figure 3 we consider all 14 solar cycles of the 3 hr *aa* index [Mayaud, 1972]. We aim to characterise extreme space weather events, but since *aa* is a coarse grained measure [Bubenik & Fraser-Smith, 1977] its maximum excursions are not well resolved [Chapman et al., 2019]. Rather than plot poorly resolved *aa* maximum values, we flag (non-overlapping) calendar days in which any of the 3hr *aa* index records in a given day exceeds a given threshold. The outer rings of Figure 2 (black dots) plot these flagged days with successively increasing radius for increasing threshold, $aa > 100, 200, 300, 400, 500, 600nT$. Radial 'spokes' on this plot then indicate severe space weather events where multiple thresholds are simultaneously exceeded.

As expected, severe events are clustered more towards solar maximum. However the clock provides more quantitative detail on how the solar cycle orders solar coronal activity and severe space weather. We see that the average terminator time (phase) identifies a clear 'switch on', that is, an increase in solar flare and severe space weather occurrence as we move from minimum to maximum in each cycle. Terminators have previously been identified solely from observations of solar coronal activity as the start time of each solar cycle, here we see the corresponding response in geomagnetic activity. Furthermore as we move from maximum to minimum, there is a decrease or 'switch off' in solar flare rates and severe space weather activity for which we will introduce the terminology 'pre-terminator'. The 'switch on' at the average terminator location occurs at a phase difference following average minimum of $\alpha = 1.2769$ radians (2.23 normalised years). We locate the pre-terminator at approximately the same phase difference preceding the average solar minimum on the solar cycle clock. We then see that between the pre-terminator, and the terminator, there is a significantly lowered occurrence rate for severe storms, only one $aa > 500nT$ and a further two $aa > 300nT$ events occurred in the entire 151 year *aa* record. This identifies a specific 'quiet interval' of the solar cycle which begins approximately $\alpha \simeq 2\pi/5$ (or 2.2 normalized years) before, and ends approximately $\alpha \simeq 2\pi/5$ (or 2.2 normalized years) after the 18 cycle average phase of solar minimum as indicated by the the blue lines on the clock, these can be seen to closely coincide with the terminator and pre-terminator. The terminator time, estimated from solar observations, then is potentially a tool to support operational decision making as it flags an imminent increase in the likelihood of more severe space weather activity. The sunspot number analytic phase can in principle be extrapolated forward in time, albeit with some uncertainty, to forecast when a specific phase will occur, such as that of the terminator for the start of the next solar cycle [Leamon et al., 2019]. From the sun clock we have determined the daily sunspot record analytic phases of both the 'switch off' and 'switch on' of severe space weather activity so that their occurrence times could both be forecast-able.

3.2 Quantifying solar cycle modulation of the level of activity.

To quantify solar coronal activity and occurrence rates of space weather of different severity, in Figure 4 we plot the same information shown on the sun clocks as histograms. The abscissa plots the $[0 - 2\pi]$ of phase on the sun clock as a normalized 11 year cycle, with year zero at the average terminator occurrence time (phase). We again form histograms of occurrences as counts in 3 month non-overlapping bins within this 11 year cycle from the entire observational record for each quantity. The top two panels (a) and (b) plot the counts per 3 month bin of the number of days, during the full *aa* record since 1868, in which *aa* exceeds the above thresholds. Panels (c) and (d) count the number of C, M and X flares per 3 month bin that were observed over the GOES catalog since 1975. The last panel (e) plots the F10.7 index (the solar radio flux at 10.7 cm) which is com-

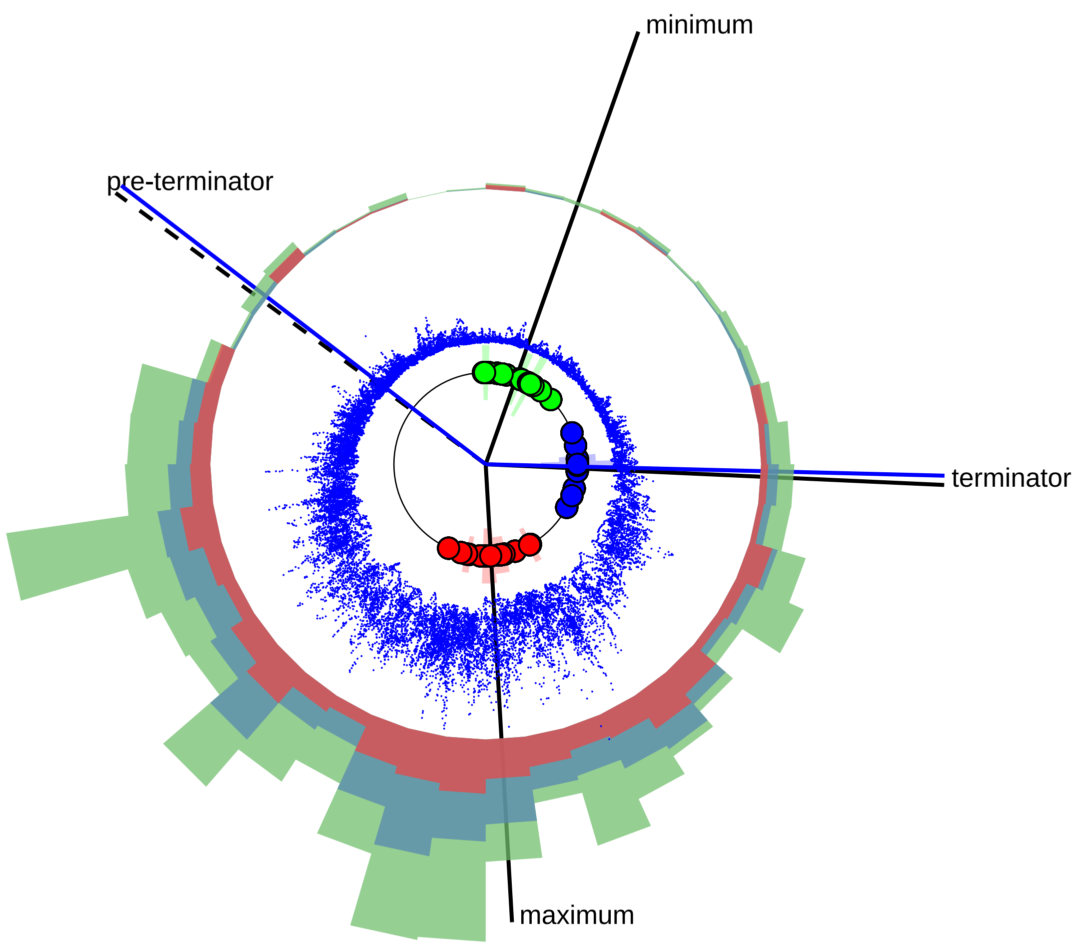

Figure 2. Increasing time (analytic phase) is read clockwise. The analytic phases of the maxima and minima of the last 18 solar cycles are indicated by red and green circles respectively and the blue circles indicate terminators for the last 12 solar cycles [McIntosh et al., 2019]. Black lines indicate the average analytic phase for the maxima, minima and terminators. The pre-terminator (dashed black line) is at the same phase difference (clock angle) in advance of the minimum as that phase difference by which the terminator lags the minimum. These phase differences are close to $\pm 2\pi/5$ either side of the average minimum phase, these are indicated by blue lines. Blue dots overplot daily F10.7 and overplotted red, blue and green histograms show counts in non-overlapping 3-month long bins for X-class, M-Class and C-class flare occurrence (scaled relative to each other in ratio 75:500:2000).

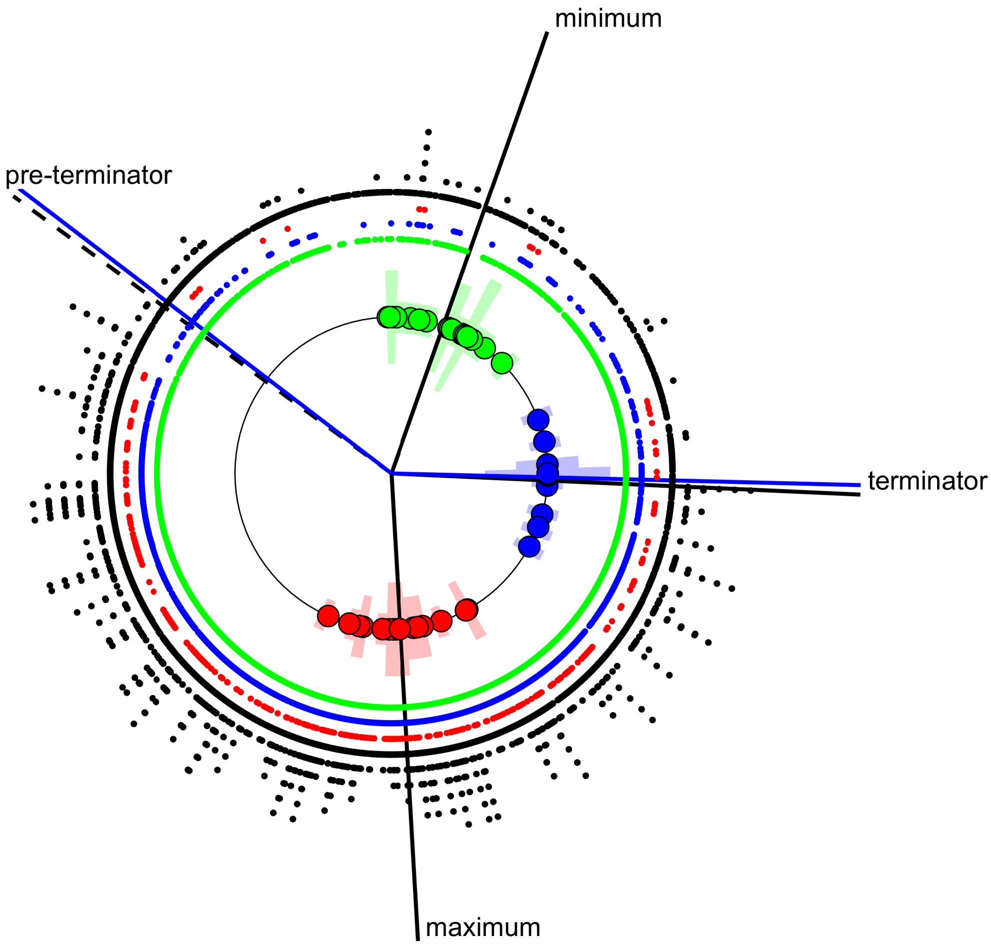

Figure 3. Increasing time (analytic phase) is read clockwise. The analytic phases of the maxima and minima of the last 18 solar cycles are indicated by red and green circles respectively and the blue circles indicate terminators for the last 12 solar cycles [McIntosh et al., 2019]. Black lines indicate the average analytic phase for the maxima, minima and terminators. The pre-terminator (dashed black line) is at the same phase difference (clock angle) in advance of the minimum as that phase difference by which the terminator lags the minimum. These phase differences are close to $\pm 2\pi/5$ either side of the average minimum phase, these are indicated by blue lines. Black dots arranged on concentric circles where increasing radius indicates *aa* values which in any given day exceeded $100, 200, 300, 400, 500, 600nT$. Red, blue and green dots indicate days in which X-class, M-Class and C-class flares respectively occurred.

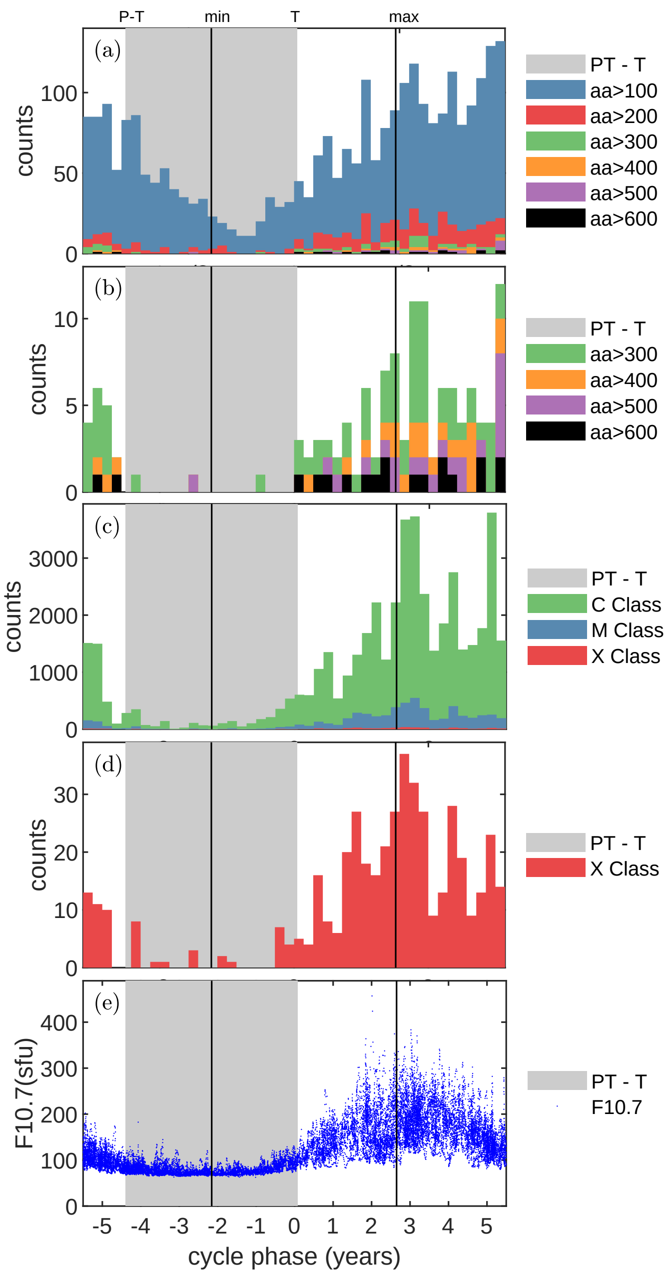

Figure 4. The abscissa plots the 2π in phase of a solar cycle on an 11 year timebase with year zero at the terminator. The average phase of solar maximum and minimum are indicated by vertical black lines. The average terminator and pre-terminator demarcate a quiet phase centred on minimum (shaded grey region). The ordinates are histogram counts of number of days in non-overlapping 3-month long bins in which (a) *aa* values exceeded $100, 200, 300, 400, 500, 600nT$ and (b) *aa* values exceeded $300, 400, 500, 600nT$; (c) counts of C and M class and (d) X Class flares. Panel (e) plots the daily F10.7 versus analytic phase obtained by Hilbert transform of the time series.

monly used as an indicator of the state of the corona. We overplot all individual records of F10.7, the index is available since 1947 giving 6 overplotted solar cycles. This data quantifies the relative occurrence likelihood of flares, and of severe space weather events, in the quiet interval compared to the solar cycle as a whole and this is detailed in Table 1.

On the 11 year normalized cycle shown in Figure 4 we indicate with a grey shaded region the quiet interval of the cycle, that is centred on the average location of solar minimum and demarcated by the pre-terminator (at -4.4 years) and terminator (at year zero) as obtained from the sun clock (Figures 2 and 3). The quiet interval clearly coincides with reduced occurrence rates for flares and severe space weather, and low values of F10.7 solar radio flux. Indeed, only 12 of the 453 X-flares from the GOES flare catalog occurred when F10.7 was < 90 sfu (Leamon et al., 2020, in preparation). Including weaker flares, only $\sim 4-6\%$ of all X, M or C flares occurred in the quiet interval; the relative chance of a flare occurring in the quiet interval is roughly the same for all flare classes. Over the 14 solar cycles of the *aa* index record there were 19 occurrences of the most intense, $aa > 600nT$ events and none of these occurred in the quiet interval. There were 3 events with $aa > 300nT$, one of which reached $aa > 500nT$ in the quiet interval, $\sim 1-3\%$ of all $aa \sim 300-500nT$ days occurred in the quiet interval. This significantly modulates solar cycle averaged estimates of the occurrence rates of severe geomagnetic storms. If the occurrence rates were uniform across the solar cycle, a quiet interval of 4.4 years within an 11 year cycle would translate to 40% of all events occurring in the quiet interval.

From 14 cycles of *aa* index data we find that more moderate storm days are less strongly modulated by the solar cycle, with $\sim 22\%$ of $aa > 100nT$ days occurring in the quiet interval. This is consistent with previous estimates based on the last 5 solar cycles. More moderate storms are more frequent and hence an estimate of the solar cycle modulation of their occurrence rates can be attempted using observations over fewer solar cycles for which there are geomagnetic indices (such as D_{ST}) that are well resolved in amplitude so that individual storms and their peak disturbance values can be identified. Based on the 5 solar cycles of available D_{ST} observations a solar cycle modulation of storm occurrence rate of a factor of 2-3 between solar maximum and minimum has been estimated [Tsubouchi & Omura, 2007]. Extrapolating distributions sorted by solar maximum and minimum to the most extreme events [Riley & Love, 2016] gives an occurrence likelihood that is more strongly solar cycle modulated, with 1.4% during solar minimum conditions and 28% in solar maximum conditions. This is again consistent with our findings however the analysis presented here does not require the assumption of any specific distribution or its extrapolation.

4 Conclusions

In summary, we have constructed a new solar cycle clock by using the daily sunspot number record to map the variable duration solar cycle onto a uniform $[0-2\pi]$ interval of analytic phase. We have found that this clearly identifies a ~ 4.4 year quiet interval centred on solar minimum in a (normalized) 11 year cycle. The start and end of this quiet interval occur at specific phases which in principle are forecast-able in real time by forwards extrapolation of the relationship between time and analytic phase of the daily sunspot number. Since F10.7 solar radio flux is also modulated by the solar cycle analytic phase, it could provide an additional signal with which to make this forecast.

Knowing when the next quiet interval will start and end has considerable implications for planning resilience of systems to the impacts of severe space weather events. Approximately $1-3\%$ of all $aa \sim 300-500nT$ days in the *aa* record occurred in solar cycle quiet intervals. This translates to a return period of $\sim 20-60$ years in quiet intervals, as compared to $\sim 0.7-2.5$ years in active intervals, whereas if it is averaged over the solar cycle the return period is $\sim 1-4$ years. The overall occurrence frequency found here

	quiet	total	quiet	active	average	
	Counts	Counts	$R(days)$	$R(days)$	$R(days)$	% quiet
occurrences	C_q	C_T	$14 \times 4.4/C_q$	$14 \times 6.6/C_a$	$151/C_T$	$C_q/C_T \times 100$
X Class	27	453	231.8 ± 44.6	22.0 ± 1.1	34.5 ± 1.62	5.9 ± 1.2
M Class	269	5965	23.3± 1.4	1.6± 0.021	2.6± 0,03	4.5±0.28
C Class	2752	45927	2.27± 0.043	0.22 ±0.001	0.34±0.002	6.0 ±0.12
	Counts	Counts	$R(yr)$	$R(yr)$	$R(yr)$	% quiet
active days	C_q	C_T	$14 \times 4.4/C_q$	$14 \times 6.6/C_a$	$151/C_T$	$C_q/C_T \times 100$
$aa > 600nT$	0	19	>151	5.3±1.2	7.95±1.8	-
$aa > 500nT$	1	40	61.6	2.4±0.38	3.78±0.6	2.5
$aa > 400nT$	1	64	61.6	1.5±0.18	2.36±0.3	1.6
$aa > 300nT$	3	130	20.5±11.9	0.73±0.065	1.16±0.10	2.3 ±1.4
$aa > 200nT$	37	426	1.67±0.27	0.24±0.012	0.35±0.017	8.7 ±1.5
$aa > 100nT$	617	2820	0.10± 0.004	0.042 ±0.001	0.054±0.001	21.9 ±1.0

Table 1. Occurrence counts and corresponding return periods R for GOES catalog flares and *aa* index active days. Over the entire data record (*aa* index since 1868 and GOES flare catalog since 1975) there are C_q counts in the quiet interval, C_a in the active interval, and $C_a + C_q = C_T$ in total. Standard errors are given.

during active intervals is just under a factor of two higher than that estimated from a solar cycle average. It is however significantly reduced during quiet intervals.

Across the *aa* record, we find that the occurrence rate of severe events is significantly more strongly solar cycle modulated than more moderate ones. Estimates of the likely occurrence rate based on more frequently occurring, moderate events may therefore underestimate the solar cycle modulation of more severe events. This pattern is not seen as strongly in the solar cycle modulation of solar flares where we find that the proportion that occur in the quiet interval is roughly the same for C, M and X class flares. This may reflect the fact that more severe geomagnetic storms tend to be more directly correlated with flare activity, whereas more moderate storms can result from other drivers in the solar wind such as high speed streams.

Data availability: The *aa* index dataset analysed here is available from the International Service of Geomagnetic Indices at http://isgi.unistra.fr/.
The daily sunspot number dataset is available from the SILSO, World Data Center - Sunspot Number and Long-term Solar Observations, Royal Observatory of Belgium, on-line Sunspot Number catalogue: http://www.sidc.be/silso/datafiles.
The dates of solar cycle maxima and minima are as determined from the smoothed sunspot number record by SILSO: http://www.sidc.be/silso/cyclesmm.
The solar radio flux at 10.7 cm (the F10.7 index) is available since 1947 at:
ftp://ftp.ngdc.noaa.gov/STP/space-weather/solar-data/solar-features/solar-radio/noontime-flux/penticton/.
The GOES X-ray Flare dataset was prepared by and made available through the NOAA National Geophysical Data Center (NGDC):
https://www.ngdc.noaa.gov/stp/space-weather/solar-data/solar-features/solar-flares/x-rays/

Acknowledgments

The results presented in this paper rely in part on geomagnetic indices calculated and made available by ISGI Collaborating Institutes from data collected at magnetic observatories. We acknowledge the involved national institutes, the INTERMAGNET network and ISGI (isgi.unistra.fr). We thank the World Data Center for Geomagnetism, Kyoto. We thank the World Data Center SILSO, Royal Observatory of Belgium, Brussels for provision of sunspot data.

SCC acknowledges a Fulbright-Lloyd's of London Scholarship and AFOSR grant FA9550-17-1-0054 and ST/P000320/1. SCC, NWW and RJL appreciate the support of the HAO Visitor Program. RJL acknowledges support from NASA's Living With a Star Program.

References

Babcock, H. W., The Topology of the Sun's Magnetic Field and the 22-YEAR Cycle, Astrophys. J., (1961), 133, 572

Baker, D. N., Lanzerotti, L. J., Resource Letter SW1: Space weather, Am. J. Phys. 84, 166 (2016) doi:10.1119/1.4938403

Bartels, J., Heck, N. H., Johnston, H. F. (1939) The three-hour-range index measuring geomagnetic activity, J. Geophys. Res., doi:10.1029/TE044i004p00411

Boashash, B. Estimating and Interpreting the Instantaneous Frequency of a Signal. Proc. IEEE®. Vol. 80(4), 1992, pp. 520-568.

Bubenik, D. M., Fraser-Smith, A. C., (1977) Evidence for strong artificial components in the equivalent linear amplitude geomagnetic indices, J. Geophys. Res., 82, 2875

Chapman, S. C., P. T. Lang, R. O. Dendy, L. Giannone, N. W. Watkins, (2018) ASDEX Upgrade Team, Control system-plasma synchronization and naturally occurring edge localized modes in a tokamak Phys. Plasmas 25, 062511 doi:10.1063/1.5025333

Chapman, S. C., Watkins, N. W., Tindale, E., (2018) Reproducible aspects of the climate of space weather over the last five solar cycles, Space Weather doi:10.1029/2018SW001884

Elvidge, S., Angling, M. J., Using Extreme Value Theory for Determining the Probability of Carrington-Like Solar Flares, (2018) doi:10.1002/2017SW001727

Chapman S. C., Horne, R. B., Watkins, N. W. Using the *aa* index over the last 14 solar cycles to characterize extreme geomagnetic activity, Geophys. Res. Lett, submitted (2019) doi: 10.1002/essoar.10501379.1

Gabor, D. "Theory of Communication." J. IEE (London). Vol. 93(3), 1946, pp. 429-441.

Hapgood, M. (2019). The great storm of May 1921: An exemplar of a dangerous space weather event. Space Weather, 17, 950–975.

Hathaway, D. H., (2015) The solar cycle, Living Rev. Solar Phys., 12, 4 doi:10.1007/lrsp-2015-4

Leamon R. J., et al., Timing Terminators: Forecasting Sunspot Cycle 25 Onset, Solar Physics, submitted (2019); arXiv:1909.06603 [astro-ph.SR]

Lockwood M., Owens, M. J., Barnard, L. A., Scott, C. J., Watt, C. E., Bentley, S., J. Space Weather Space Clim., 8, A12, (2018) Space climate and space weather over the past 400years: 2. Proxy indicators of geomagnetic storm and substorm occurrence, doi:10.1051/swsc/2017048

Marple, S. L. (1999) "Computing the Discrete-Time Analytic Signal via FFT." IEEE® Transactions on Signal Processing. Vol. 47, , pp. 2600–2603.

Mayaud, P-N. (1972) The aa indices: A 100 year series characterizing the magnetic activity, J. Geophys. Res., 77, 6870

Mayaud, P. N. (1980). Derivation, Meaning, and Use of Geomagnetic Indices, Geophys. Monogr. Ser., vol. 22, AGU, Washington, D.C. doi:10.1029/GM022

McIntosh, S.W., Leamon, R.J. (2014 a) On Magnetic Activity Band Overlap, Interaction, and the Formation of Complex Solar Active Regions. Astrophys. J. Lett. 796, L19

McIntosh, S.W., Wang, X., Leamon, R.J., Scherrer, P.H.: (2014 b) Identifying Potential Markers of the Sun's Giant Convective Scale. Astrophys. J. Lett. 784, L32.

McIntosh, S.W., Leamon, R.J., Egeland, R., Dikpati, M., Fan, Y., Rempel, M. (2019), What the sudden death of solar cycles can tell us about the nature of the solar interior. Solar Physics 294 (7), 88. doi:10.1007/s11207-019-1474-y

Oughton, E., Copic, J., Skelton, A., Kesaite, V., Yeo, Z. Y., Ruffle, S. J., Tuveson, M., Coburn, A. W., Ralph, D. Helios (2016) Solar Storm Scenario, Cambridge Risk Framework series, Centre for Risk Studies, University of Cambridge

Oughton et al (2017), Quantifying the daily economic impact of extreme space weather due to failure in electricity transmission infrastructure, Space Weather,15,65–83

Palŭs, M., Notovná, D. (1999) Sunspot Cycle: A Driven Nonlinear Oscillator?, PRL, 83, 3406

Riley, P. (2012). On the probability of occurrence of extreme space weather events, Space Weather 10, S02012.

Riley, P., Love, J. J., (2016) Extreme geomagnetic storms: Probabilistic forecasts and their uncertainties, Space Weather, 15, 53–64, doi:10.1002/2016SW001470.

Russell, C. T., L. K. Jian, J. G. Luhmann,(2019) The solar clock, Rev. Geophys. doi:10.1029.2019RG000645

Sheeley, N. R., Wang, Y.-M. & Harvey, J. W., The Effect of Newly Erupting Flux on the Polar Coronal Holes, Sol. Phys., (1989) 119, 323.

Silbergleit, V. M. (1996) On the occurrence of geomagnetic storms with sudden commencements, J. Geomagn. Geoelectr., 48, 1011.

Silbergleit, V. M. (1999) Forecast of the most geomagnetically disturbed days, Earth Planets Space, 51, 19

Siscoe, G. L., (1976) On the statistics of the largest geomagnetic storms per solar cycle, J. Geophys. Res., 81, 4782

Tapping, K. F. (2013). The 10.7 cm solar radio flux (F10.7), Space Weather, 11, 394. doi:10.1002/swe.20064

Thomson, A. W. P., Gaunt, C. T., Cilliers, P., Wild, J. A., Opperman, B., McKinnell, L.-A., Kotze, P., Ngwira, C.M., Lotz, S.I., (2010) Present day challenges in understanding the geomagnetic hazard to national power grids Adv. Space Res. 45 1182–1190 doi:10.1016/j.asr.2009.11.023

Thomson, A. W. P, Dawson, E. B., Reay, S. J., Quantifying extreme behaviour in geomagnetic activity, Space Weather, 9, S10001, (2011) doi:10:1029/2011SW000696

Tsubouchi, K., Omura, Y., Long-term occurrence probabilities of intense geomagnetic storm events, Space Weather, 5, S12003, (2007) doi:10.1029/2007SW000329

Tsurutani, B. T., Gonzalez, W. D., Lakhina, G. S., Alex, S., (2003) The extreme magnetic storm of 1-2 September 1859, J. Geophys. Res., 108(A7), 1268, doi:10.1029/2002JA009504

Tsurutani, B. T., et al. (2006) Corotating solar wind streams and recurrent geomagnetic activity: A review, J. Geophys. Res., 111, A07S01, doi:10.1029/2005JA011273.

Vedder, J. D., & Tabor, J. L. (1992). Solar F10.7 Radiation: A Short-Term Statistical Model, J. Spacecraft and Rockets, 29, 76. https://doi.org/10.2514/3.26316